

# Broadband Shock Noise from Supersonic Jets

T. D. Norum\* and J. M. Seiner\*  
*NASA Langley Research Center, Hampton, Va.*

Broadband shock noise from supersonic jets is investigated through acoustic measurements in both the near and far fields. The peak Helmholtz number of broadband shock noise from unheated convergent nozzles is found to be independent of nozzle pressure ratio when based on the length of the shock cells and the ambient speed of sound. Excellent agreement between power spectral densities measured at various far-field angles is obtained at and above the peak shock noise frequency when source convection and directivity effects are included. The directivity of broadband shock noise is found to be pointed in the upstream direction, with omnidirectionality being approached only at high pressure ratios. For both convergent and convergent-divergent nozzles, the relative importance of shock noise with respect to jet-mixing noise is found to be maximum near the pressure ratio at which a Mach disk begins to form in the jet. Near-field measurements point to a limited portion of the shock cell system as the region of dominant broadband noise emission from a highly underexpanded convergent nozzle.

## Nomenclature

$c_0$	= ambient speed of sound
$d$	= nozzle exit diameter
$D$	= Doppler factor, $1 + M_c \cos \psi$
$f_p$	= peak emission frequency of broadband shock noise
$L$	= average shock cell spacing
$M_c$	= convection Mach number, $U_c/c_0$
$M_j$	= fully expanded Mach number
$n$	= number of Doppler factors in shock noise directivity
$p_a$	= ambient static pressure
$p_e$	= nozzle exit static pressure
$p_s$	= static pressure in jet
$p_t$	= jet stagnation pressure
$U_c$	= eddy convection velocity
$U_j$	= fully expanded jet velocity
$x$	= distance from nozzle exit
$\beta^2$	= $M_j^2 - 1$
$\lambda_p$	= wavelength of peak shock noise, $c_0/f_p$
$\psi$	= far-field angle measured from jet inlet

## Introduction

THE noise produced due to the presence of shock waves in a supersonic jet has direct application to the future design of commercial supersonic aircraft exhaust nozzles. A comprehensive program to investigate both aerodynamic and associated acoustic phenomena of shock containing jets has been undertaken at NASA Langley Research Center. Some of the major results of these measurements are presented in this paper.

Shock noise from supersonic jets can contain two components. The first consists of high-amplitude discrete tones, called screech, which was first studied by Powell.<sup>1</sup> He inferred the mechanism of screech generation to be a resonant loop consisting of acoustic feedback of noise generated by the passage of disturbances through a shock that resulted in additional disturbances being created at the nozzle exit. Powell modeled screech as a succession of stationary point sources located at the shock positions with phase differences determined from the convection velocity of the disturbances.

The resulting predicted directivities of both the fundamental screech frequency and its harmonic agree well with observations. Lassiter and Hubbard<sup>2</sup> investigated the motion of the primary shock at a condition of strong screech and found it to oscillate at the frequency of the fundamental screech tone. These indications that the source of screech is spatially stationary are well borne out by the fact that measured screech frequencies are independent of observer position.

The second component of shock noise is broadband in nature. Its spectrum amplitude rises rapidly with frequency to a well-defined peak and then decreases at higher frequency. This broadband shock-associated noise is in general easily distinguishable from the lower frequency jet-mixing noise, and it exhibits a frequency shift with measurement angle indicative of a Doppler effect. Harper-Bourne and Fisher<sup>3</sup> were the first to investigate this noise source in detail, and suggested a mechanism based on an extension of Powell's model for screech. Their Schlieren measurements with an underexpanded convergent nozzle showed strong fluctuations within the shear layer of the jet at the end of each shock cell as well as good correlation between neighboring cells. The amplitude of the fluctuations varied with nozzle exit pressure in the same manner as did the radiated sound field. This led to a model of stationary acoustic sources positioned at the end of each shock cell with the apparent Doppler shift being accounted for by the relative phasing of the sources. The peak Strouhal number (based on the peak frequency of the broadband noise, the shock cell spacing, and the eddy convection velocity) was predicted to be unity.

Howe and Ffowcs Williams<sup>4</sup> proposed a theoretical model of the broadband shock noise process in which energy is extracted from the ordered nonuniform mean flow of the jet and redistributed into random scattered disturbances. The peak of the noise spectrum is associated with the coherent scattering of sound by the array of shock cells, with additional sound waves produced through multiple scattering forming the wide frequency range of the broadband noise. Their predicted peak frequency is also dependent on eddy convection velocity and shock spacing, with the shear layer velocity producing an actual rather than an apparent Doppler effect.

This paper presents experimental results aimed at enhancing current techniques for modeling broadband shock noise from supersonic jets. Extensive measurements of jet plume static pressure and far-field acoustic pressure were obtained for unheated jets from both convergent and convergent-divergent (C-D) nozzles. The relationship between shock cell spacing and broadband shock noise peak frequency

Presented as Paper 80-0983 at the AIAA 6th Aeroacoustics Conference, Hartford, Conn., June 4-6, 1980; submitted Nov. 4, 1980; revision received July 27, 1981. This paper is declared a work of the U.S. Government and therefore is in the public domain.

\*Research Engineer, Acoustics and Noise Reduction Division, Member AIAA.

is demonstrated, as is the directivity of shock noise and the similarity of the radiation from the different types of nozzles. In addition, the region of dominant noise emission for a highly underexpanded convergent nozzle is estimated from near-field acoustic measurements.

### Experimental Apparatus

The far-field acoustic measurements reported herein were performed in the NASA Langley Research Center Anechoic room with interior dimensions of  $6.71 \times 8.43 \times 7.23$  m. Eighteen  $\frac{1}{4}$  in. free-field condenser microphones were used, located at 7.5 deg intervals on a radius of 3.66 m between 30 and 157.5 deg with respect to the upstream jet axis. The remainder of the data were obtained in the NASA Langley jet noise aerodynamics facility. The near-field noise measurements consisted of traversing a  $\frac{1}{8}$  in. condenser microphone parallel to the jet centerline at a radial distance of 14 cm. All acoustic data were recorded on an FM magnetic tape recorder. Details of both facilities are described in Ref. 5.

Three different nozzles were constructed and used in this study. The first is a convergent nozzle of exit diameter 3.90 cm which was designed for parallel flow at the nozzle exit. The other two were convergent-divergent (C-D) nozzles, one designed for an exit Mach number of 1.5 with an exit diameter of 4.27 cm, and the other designed for Mach number 2.0 with a diameter of 4.99 cm. The diameters were chosen so that the convergent nozzle would produce the same ideal thrust as the others at their respective design conditions.

The interaction between screech and broadband shock noise is unclear at this time. It is generally assumed that the two are independent and that broadband shock noise can be studied by eliminating the discrete components of screech. Tanna<sup>6</sup> was very successful in eliminating screech for a convergent nozzle by covering the nozzle interior with sound-absorbing material and inserting a small projection (tab) into the jet at the nozzle exit. Tabs based on Tanna's design (extending  $0.063 d$  into the flow and  $0.125 d$  wide) were constructed for each of the nozzles used in the current experiments. Tests were performed both with and without a tab, and the results from each are used where appropriate.

The range of supersonic nozzle pressure ratios  $p_t/p_a$  tested was 1.9-14.0. These are reported in terms of the parameter  $\beta$ , where  $\beta^2 = M_j^2 - 1 = 5(p_t/p_a)^{2/7} - 6$  for air.  $\beta^2$  is proportional to the pressure rise across a normal shock of approach Mach number  $M_j$ . Harper-Bourne and Fisher<sup>3</sup> found that this parameter correlated broadband shock noise quite well up to the formation of a Mach disk in the jet.

### Shock Cell Spacing and Broadband Noise Peak Frequency

Static pressure measurements within the jet plume were made using the supersonic static pressure probe described in Ref. 5. An average shock cell spacing was determined from axial traverses over a wide range of pressure ratios for each nozzle. For the convergent nozzle the average spacing was found to vary as  $\bar{L}/d = 1.1\beta$ , which is the same as that obtained by Harper-Bourne and Fisher<sup>3</sup> from laser-Schlieren measurements. Although the variation of cell spacing for C-D nozzles is more complicated, an excellent correlation was obtained in the form  $\bar{L}/d = a\beta^b$ , where  $a = 1.1$ ,  $b = 1.17$  for the Mach 1.5 nozzle and  $a = 0.75$ ,  $b = 1.63$  for the Mach 2 nozzle.

Introduction of a tab at the nozzle lip influences the development of the shock structure within the jet. Figure 1 shows the centerline variation of static pressure over the first four shock cells at  $\beta = 0.94$  for the convergent nozzle with and without a tab. The tab gives steeper compression regions with a resultant shortening of the shock cell lengths by about 10%. Similar comparisons show this same percentage decrease, yielding an average shock cell spacing for the convergent nozzle with tab varying as  $\bar{L}/d = 1.0\beta$ .

Preliminary examination of the peak frequency of

broadband shock noise showed that the Strouhal number  $f_p \bar{L}/U_c$  has a tendency to decrease with increasing pressure ratio,<sup>5</sup> contrary to the theoretical predictions. On the other hand, the Helmholtz number  $f_p \bar{L}/c_0$  appeared to be constant. Hence, it was decided to investigate the apparent independence of peak frequency and eddy convection velocity in more detail.

Since a tab effectively eliminates screech tones at most conditions, the narrow-band peak frequency of the broadband shock noise from the convergent nozzle with tab is easily recognized. Shown in Fig. 2 is the wavelength of the peak noise against the cosine of the far-field angle. Data are shown for all conditions at which the peak frequency was discernible. The straight line variations show the well-known Doppler shift with angle. The slopes of the least square straight lines yield a convection velocity  $U_c/U_j = 0.70 \pm 0.04$ , again in good agreement with the measurements of Harper-Bourne and Fisher.<sup>3</sup>

Similar computations of tab-free conditions show considerably more scatter, since the presence of screech tones in the spectra make detection of the peak broadband shock noise more difficult. Hence in the results to follow, the convection velocity was chosen as 70% of the fully expanded velocity at all conditions. Peak emission frequencies were then computed as  $f_p = f_\psi(1 + M_c \cos \psi)$ , where  $f_\psi$  is the measured peak at the far-field angle  $\psi$ .

Variations of both Strouhal and Helmholtz numbers for the convergent nozzle with tab are given in Fig. 3a along with the least squares straight line fits. Multiple points at a given operating condition correspond to different far-field angles. The decrease in the Strouhal number with increasing pressure ratio is obvious. The Helmholtz number is relatively invariant and has a value close to unity. Computations based on the spectra obtained by Tanna et al.<sup>7</sup> are shown in Fig. 3b and give almost identical results.

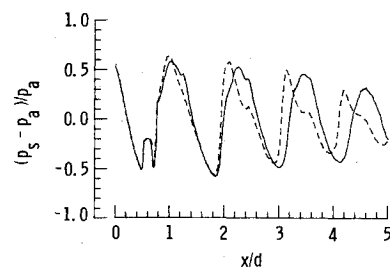


Fig. 1 Static pressure along jet centerline of convergent nozzle at  $\beta = 0.94$ : — no tab, --- with tab.

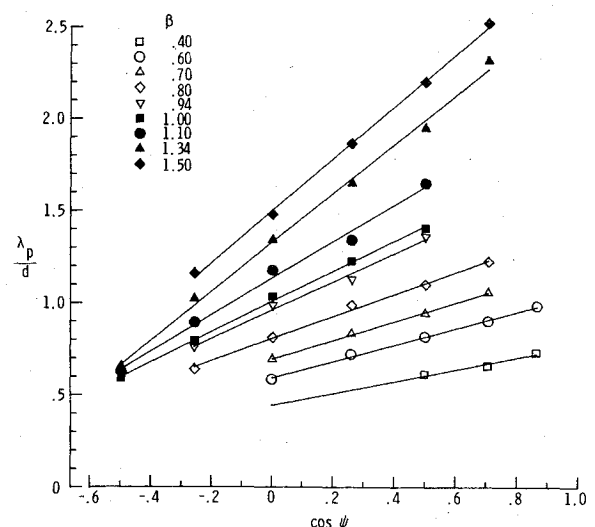


Fig. 2 Measured wavelength of peak broadband shock noise of convergent nozzle with tab.

Similar trends for the tab-free convergent nozzle can be seen in Fig. 4a. The considerable scatter at a given pressure ratio is indicative of the difficulty of peak frequency identification mentioned above. Again, it is the Helmholtz number rather than the Strouhal number that is relatively independent of  $\beta$ . Figure 4b shows results obtained from the measured peak frequencies at 90 deg given in Fig. 10 of Ref. 3. The agreement between the two sets of data is apparent.

Strouhal and Helmholtz number variations for the C-D nozzles are presented in Fig. 5. The behavior of the Mach 1.5 nozzle is very similar to that of the convergent nozzles, but the Helmholtz number of the Mach 2 nozzle shows an apparent increase with pressure ratio. The reason for this difference is unknown; the major operational difference between the nozzles is that the Mach 2 nozzle is overexpanded over most of the pressure ratio range tested.

The least squares straight lines shown in Figs. 3-5 can be expressed as  $N = N_0 + m\beta$ , where  $N$  represents either the Strouhal or Helmholtz number. Values for the intercept and slope of these lines are summarized in Table 1. As discussed above, the slopes of the lines show the relative insensitivity of the Helmholtz number to operating conditions for all but the Mach 2 nozzle. The differences in the intercepts between the nozzle configurations suggest the value of the Helmholtz number may depend on nozzle exit conditions. The fact that the Helmholtz number is approximately unity or slightly smaller indicates that the longest wavelengths of the broadband shock noise from unheated jets are limited by the shock cell spacing.

It should be mentioned here that the measured peak frequencies of broadband shock noise from heated jets are noticeably higher than those from cold jets. However, it is shown in Ref. 8 that both the hot and cold jet data of Tanna et

al.<sup>7</sup> yield the same Helmholtz number when the ambient sound speed is replaced by the sound speed based on total jet temperature. The two speeds are obviously the same for cold jets.

### Directivity of Broadband Shock Noise

It was demonstrated in Fig. 2 that for the convergent nozzle with tab the measured peak frequency variation with far-field angle is correlated well by the Doppler factor. To compare spectra at different angles, the measured far-field power spectral densities were shifted in frequency by this factor. This shift has the effect of stretching the spectrum in the upstream direction and compressing it downstream, so that one Doppler factor (i.e.,  $10 \log D$ ) must be subtracted from the measured levels in order to maintain comparative spectrum levels. When the spectra were reduced in this manner the peak frequencies aligned as expected, but differences in amplitudes indicated a directivity pattern to broadband shock noise pointed in the upstream direction. It was found that the amplitudes at the peak Doppler-shifted frequency could be normalized extremely well for all angles by subtracting  $n$  additional Doppler factors from the spectra levels, these additional factors then being a measure of the shock noise directivity.

Results for the spectra normalized in this manner are shown for a wide range of  $\beta$  values and angles in Fig. 6. The amplitudes near the broadband shock noise peak frequency are seen to collapse to within  $\pm 1$  dB for all angles  $\psi$  between 45 and 105 deg. A reasonable collapse of the data at higher frequencies is also noted, whereas the lower frequencies representative of jet-mixing noise are of course completely uncorrelated. The number of additional Doppler factors  $n$  necessary to perform these spectral normalizations are given

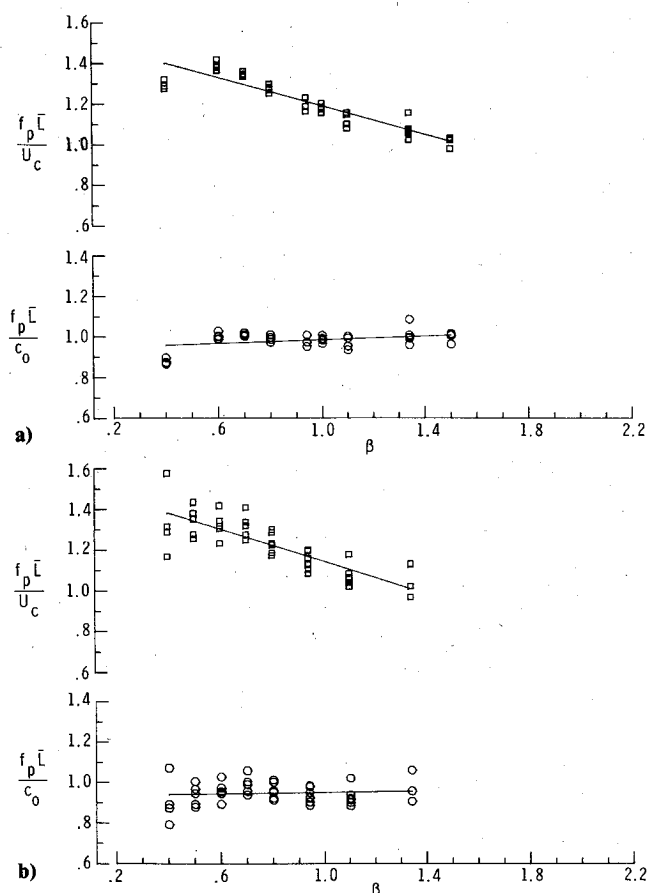


Fig. 3 Variation of Strouhal and Helmholtz numbers of broadband shock noise peak for convergent nozzle with tab: a) present test, b) Ref. 7.

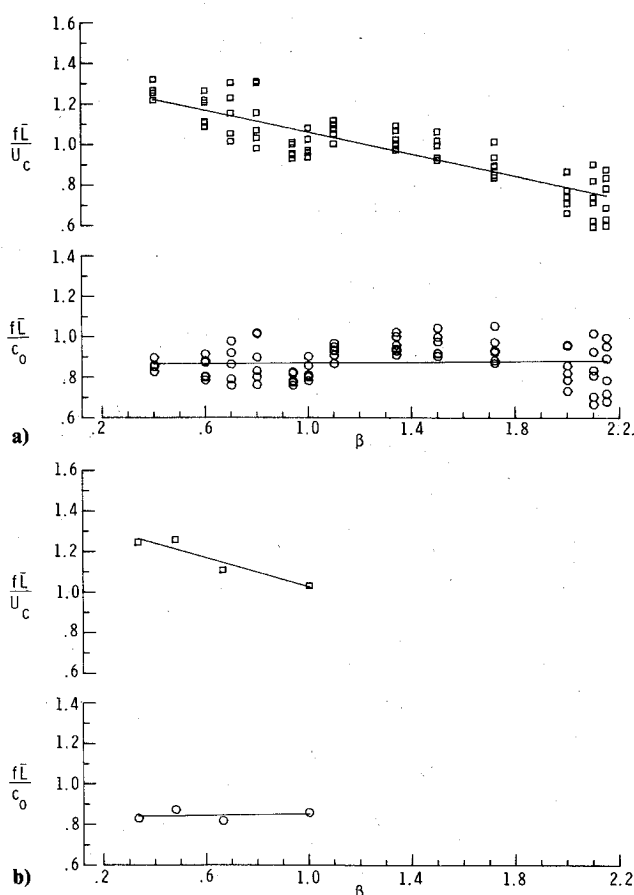


Fig. 4 Variation of Strouhal and Helmholtz numbers of broadband shock noise peak for convergent nozzle: a) present test, b) Ref. 3.

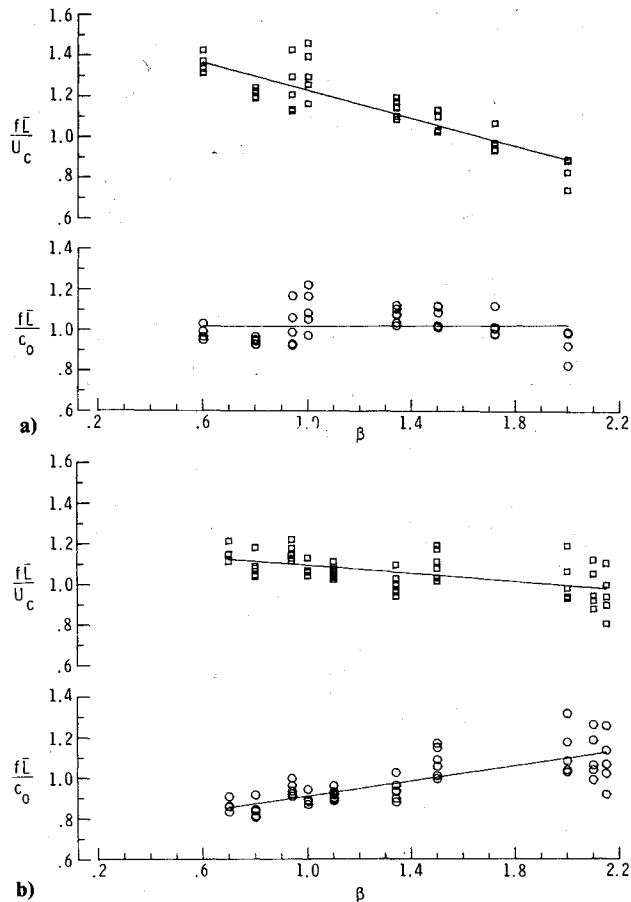


Fig. 5 Variation of Strouhal and Helmholtz numbers of broadband shock noise peak for C-D nozzles: a) Mach 1.5, b) Mach 2.

in Fig. 7. Since a value of zero for this number represents omnidirectional radiation, it can be seen that broadband shock noise is fairly directional at lower  $\beta$  values and approaches omnidirectionality only at high  $\beta$  values.

### Relative Importance of Broadband Shock Noise

As discussed in detail in Ref. 6, the relative importance of shock noise in comparison to jet noise for a convergent nozzle generally increases with increasing pressure ratio, increasing angle from the downstream jet axis, and decreasing jet temperature. An attempt to quantify this relative importance with respect to pressure ratio for each of the three nozzles was made as follows.

At each value of  $\beta$ , one-third octave spectra with and without tabs were generated. The midfrequency range of the no tab data was in many cases dominated by screech tones, whereas the high-frequency portion of the tab data contained higher noise levels generated by the presence of the tab. By choosing the lower level in each third-octave band between the two cases, a spectrum relatively free from both these phenomena was obtained.

Having spectra that could now be considered representative

Table 1 Slopes and intercepts of straight line fits

Nozzle type	Strouhal No.		Helmholtz No.	
	$N_0$	$m$	$N_0$	$m$
Convergent, with tab	1.54	-0.35	0.94	0.05
Convergent, with tab <sup>7</sup>	1.54	-0.40	0.94	0.06
Convergent	1.33	-0.27	0.86	0.01
Convergent <sup>3</sup>	1.38	-0.36	0.83	0.02
Mach 1.5	1.57	-0.33	1.01	0.01
Mach 2	1.19	-0.10	0.73	0.19

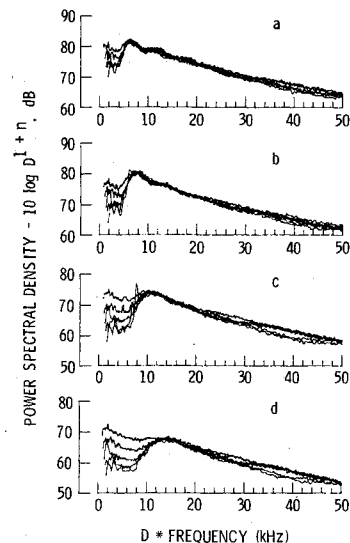


Fig. 6 Doppler shifted power spectral densities with amplitude corrections for convergent nozzle with tab at  $\psi = 45, 60, 75, 90$ , and  $105$  deg: a)  $\beta = 1.34, n = 0.5$ , b)  $\beta = 1.1, n = 1$ ; c)  $\beta = 0.8, n = 2$ ; d)  $\beta = 0.6, n = 2.5$ .

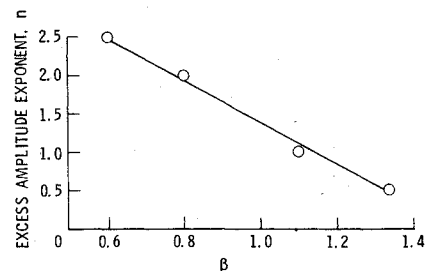


Fig. 7 Estimate of broadband shock noise directivity factor exponent.

of jet-mixing noise combined with broadband shock noise, the next step was to eliminate the effect of increasing jet noise with  $\beta$ . The range of pressure ratios and nozzle types being considered precluded an accurate functional relationship for the jet-mixing noise. However, since the low-frequency portion of the spectra at all conditions is relatively free from shock noise, this part of the spectra can be used to compute the relative increase of jet noise level with  $\beta$  at a given far-field angle. Hence, for each spectrum, the overall level consisting of the energy below 1 kHz was computed and then subtracted from each third octave band. This procedure produced corrected spectra that were normalized to roughly the same jet-mixing noise content. The accuracy of the procedure was checked by computing overall levels from the corrected spectra of the convergent nozzle at  $\psi = 150$  deg (an angle where shock noise is insignificant in comparison to mixing noise). These overall levels agreed to within  $\pm 2$  dB over the entire 0-2.15 range of  $\beta$ .

The resulting corrected one-third octave spectra for the convergent nozzle at the far-field angle of  $90$  deg are shown in Fig. 8 for a wide range of  $\beta$  values. The collapse of the low-frequency portion of these spectra is evident. The difference at the high frequencies can be attributed to broadband shock noise. An excess broadband shock noise is defined as the difference between the overall levels computed from these corrected spectra at the given operating condition and  $\beta = 0$  (the sonic condition).

Values for this excess broadband shock noise were computed for each nozzle at  $\psi = 90$  deg. They are shown in Fig. 9 vs the ratio of exit static pressure to ambient pressure. For all the nozzles operating in the underexpanded mode, the shock

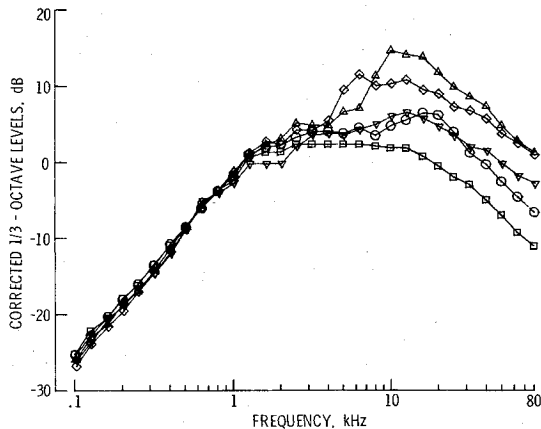


Fig. 8 Third-octave spectra of convergent nozzle at 90 deg corrected to the same jet noise level:  $\square \beta=0$ ,  $\circ \beta=0.4$ ,  $\triangle \beta=0.8$ ,  $\diamond \beta=1.34$ ,  $\nabla \beta=2.15$ .

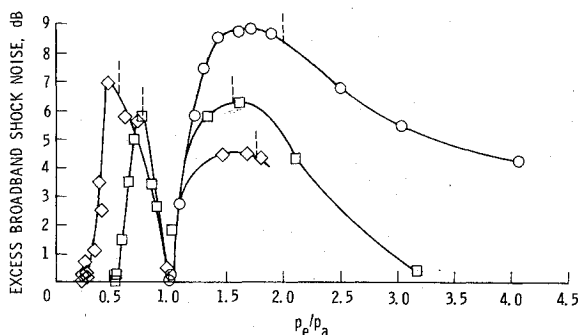


Fig. 9 Excess broadband shock noise vs static pressure at nozzle exit:  $\circ$  convergent,  $\square$  Mach 1.5,  $\diamond$  Mach 2 (dotted lines represent pressure of Mach disk formation).

noise increases from the design condition ( $p_e/p_a = 1$ ) to a maximum level between a static pressure ratio of 1.5 and 2.0, and then decreases in importance with respect to jet-mixing noise as the pressure is increased further. For the C-D nozzles operating in the overexpanded mode, a peak in the excess shock noise also occurs between the design condition and the sonic operating pressure ratio. The vertical dotted lines in Fig. 7 are the exit static pressure ratios that correspond to the beginning of Mach disk formation in the jet for each nozzle as obtained from the data of Love et al.<sup>9</sup> The peaks in the excess shock noise are seen to correspond closely to the region of Mach disk formation.

#### Location of Apparent Source of Broadband Shock Noise

A comparison of the measured strengths of the first three shock cells of underexpanded jets is given in Ref. 10. The strengths of the second and third cells reach a maximum near the pressure ratio of Mach disk formation, corresponding to the behavior exhibited by the excess broadband shock noise of Fig. 9. However, the strength of the first cell increases continuously with pressure, indicating that some shock cells may be more important than others in the broadband noise generation process.

An attempt to locate the region of the jet from which the dominant broadband noise emanates was made for the convergent nozzle at  $\beta=1.1$ . Since screech is predominant at this condition, the tab was installed. A microphone was located 3.53 nozzle exit diameters above the jet centerline and traversed axially from the nozzle exit plane to 11.7 diameters downstream. Spectra were obtained at 20 locations within the traverse.

The power spectral densities of the measurements in the near field were very similar to those obtained in the far field.

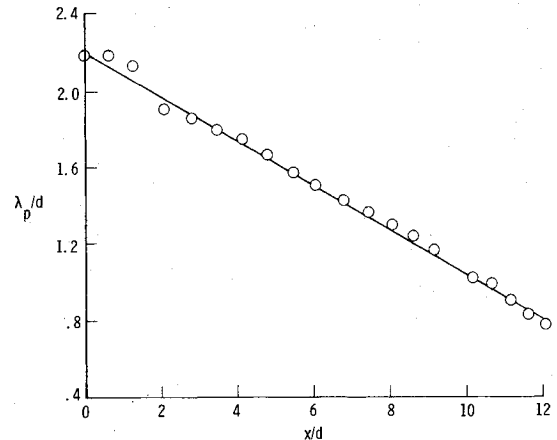


Fig. 10 Peak broadband shock noise wavelengths from near-field measurements for convergent nozzle with tab at  $\beta=1.1$ .

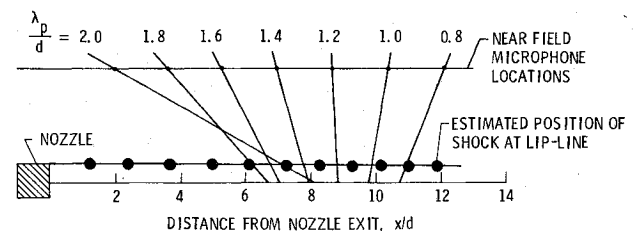


Fig. 11 Apparent source location of broadband shock noise for convergent nozzle with tab at  $\beta=1.1$ .

They contain a broadband shock noise peak that moves to higher frequency as the observation point is moved downstream, characteristic of a Doppler frequency shift. The continuous nature of this shift is shown in the peak wavelength plot of Fig. 10. Since an extensive array of similar noise sources does not produce this type of near-field variation, the source of the peak broadband noise must be limited in extent. To estimate the dominant region of emission, the positions at which a given wavelength was measured in the near and far fields were joined. The intersection of these lines of propagation with the jet are shown in Fig. 11. Also shown are the approximate positions of the shocks at the nozzle lip line. The apparent source of the broadband shock noise peak is seen to be located between 6 and 11 diameters from the nozzle exit. This corresponds to a region between the sixth and tenth shock cells at this pressure ratio. Hence, unless noise generated at the upstream shocks is carried downstream before escaping from the jet, the radiated noise appears to be generated in the region of the weaker downstream shocks. This indicates that the structure of the turbulent mixing layer is as important a variable as the shock strength in producing the dominant broadband shock noise.

#### Conclusions

The peak Strouhal number of broadband shock noise decreases with increasing pressure ratio, contrary to current theoretical predictions. Since the corresponding Helmholtz number is found to be invariant for all but the overexpanded Mach 2 nozzle, shock cell spacing is apparently the appropriate length scale that determines the broadband noise peak. The average convection velocity of the mixing layer eddies accounts for the angular variation of the measured spectra through the Doppler factor, but does not appear to be the velocity governing the peak frequency selection.

Detailed spectral comparisons at different far-field angles indicate a small but consistent directivity to broadband shock noise, with omnidirectionality being approached only at high pressure ratios. Shock noise radiation from convergent-divergent nozzles is found to be very similar to that from a

convergent nozzle, reaching maximum levels near the pressure ratio of Mach disk formation.

The dominant broadband shock noise emission from a highly underexpanded convergent nozzle appears to be located in the region of the weaker downstream shock cells. This is contrary to current prediction procedures that employ an extensive array of shock cells as significant broadband noise sources. Detailed measurements within the jet appear to be necessary in order to quantify the relationship between the shock noise process and the measured noise emission characteristics.

### References

<sup>1</sup>Powell, A., "On the Noise Emanating from a Two-Dimensional Jet Above the Critical Pressure," *Aeronautical Quarterly*, Vol. IV, Feb. 1953, pp. 103-122.

<sup>2</sup>Lassiter, L. W. and Hubbard, H. H., "The Near Noise Field of Static Jets and Some Model Studies of Devices for Noise Reduction," NACA TN 3187, July 1954.

<sup>3</sup>Harper-Bourne, M. and Fisher, M. J., "The Noise from Shock

Waves in Supersonic Jets," *Proceedings of the AGARD Conference on Noise Mechanisms*, AGARD CP-131, 1973.

<sup>4</sup>Howe, M. S. and Ffowcs Williams, J. E., "On the Noise Generated by an Imperfectly Expanded Supersonic Jet," *Philosophical Transactions of Royal Society*, Vol. 289, No. 1358, May 1978, pp. 271-314.

<sup>5</sup>Seiner, J. M. and Norum, T. D., "Experiments of Shock Associated Noise on Supersonic Jets," AIAA Paper 79-1526, July 1979.

<sup>6</sup>Tanna, H. K., "An Experimental Study of Jet Noise, Part II: Shock Associated Noise," *Journal of Sound and Vibration*, Vol. 50, 1977, pp. 429-444.

<sup>7</sup>Tanna, H. K., Dean, P. D., and Burrin, R. H., "The Generation and Radiation of Supersonic Jet Noise," *Shock Associated Noise Data*, Vol. IV, AFAPL-TR-76-65, 1976.

<sup>8</sup>Pao, S. P. and Seiner, J. M., "A Theoretical and Experimental Investigation of Shock-Associated Noise in Supersonic Jets," AIAA Paper 81-1973, Oct. 1981.

<sup>9</sup>Love, E. S., Grigsby, C. E., Lee, L. P., and Woodling, M. J., "Experimental and Theoretical Studies of Axisymmetric Free Jets," NASA TR R-6, 1959.

<sup>10</sup>Seiner, J. M. and Norum, T. D., "Aerodynamic Aspects of Shock Containing Jet Plumes," AIAA Paper 80-0965, June 1980.

*From the AIAA Progress in Astronautics and Aeronautics Series . . .*

## GASDYNAMICS OF DETONATIONS AND EXPLOSIONS—v. 75 and COMBUSTION IN REACTIVE SYSTEMS—v. 76

*Edited by J. Ray Bowen, University of Wisconsin,  
N. Manson, Université de Poitiers,  
A. K. Oppenheim, University of California,  
and R. I. Soloukhin, BSSR Academy of Sciences*

The papers in Volumes 75 and 76 of this Series comprise, on a selective basis, the revised and edited manuscripts of the presentations made at the 7th International Colloquium on Gasdynamics of Explosions and Reactive Systems, held in Göttingen, Germany, in August 1979. In the general field of combustion and flames, the phenomena of explosions and detonations involve some of the most complex processes ever to challenge the combustion scientist or gasdynamicist; simply for the reason that *both* gasdynamics and chemical reaction kinetics occur in an interactive manner in a very short time.

It has been only in the past two decades or so that research in the field of explosion phenomena has made substantial progress, largely due to advances in fast-response solid-state instrumentation for diagnostic experimentation and high-capacity electronic digital computers for carrying out complex theoretical studies. As the pace of such explosion research quickened, it became evident to research scientists on a broad international scale that it would be desirable to hold a regular series of international conferences devoted specifically to this aspect of combustion science (which might equally be called a special aspect of fluid-mechanical science). As the series continued to develop over the years, the topics included such special phenomena as liquid- and solid-phase explosions, initiation and ignition, nonequilibrium processes, turbulence effects, propagation of explosive waves, the detailed gasdynamic structure of detonation waves, and so on. These topics, as well as others, are included in the present two volumes. Volume 75, *Gasdynamics of Detonations and Explosions*, covers wall and confinement effects, liquid- and solid-phase phenomena, and cellular structure of detonations; Volume 76, *Combustion in Reactive Systems*, covers nonequilibrium processes, ignition, turbulence, propagation phenomena, and detailed kinetic modeling. The two volumes are recommended to the attention not only of combustion scientists in general but also to those concerned with the evolving interdisciplinary field of reactive gasdynamics.

Volume 75—468 pp., 6×9, illus., \$30.00 Mem., \$45.00 List  
Volume 76—688 pp., 6×9, illus., \$30.00 Mem., \$45.00 List  
Set—\$60.00 Mem., \$75.00 List

TO ORDER WRITE: Publications Dept., AIAA, 1290 Avenue of the Americas, New York, N. Y. 10104